

Finite Element Simulation of Cylinder Closure Spinning

Liyan Sui (0009-0009-3839-3886)¹, Yilian Xie (0009-0000-7316-5568)^{2*}, Baoming Liu (0009-0001-4757-041X)^{1,3}, Zhen Jia (0000-0002-2433-641X)¹

¹Faculty of Aerospace Engineering, Shenyang Aerospace University, Shenyang 110136, China

²Faculty of Mechanical Engineering, Liaoning Open University (Liaoning Equipment Manufacture College), Shenyang 110161, China

³Engineering Training Center, Shenyang Aerospace University, Shenyang 110136, China

*Corresponding Author, Yilian Xie, Liaoning Open university (Liaoning Equipment Manufacture College), Shenyang 110161, P.R. China, 3234405839@qq.com, Tel/Fax numbers: +86 24 89728200

As a gas storage container, gas cylinders have been widely used in industry, mining, military, medicine, diving, automobiles and other fields. The gas cylinder produced by spinning can fundamentally eliminate the defects related to the weld in the traditional production process. In order to explore the metal flow law of cylinder closure spinning, its finite element simulation is established and carried out by using ABAQUS/explicit software. The influence of the parameters such as angle radius R and screw wheel installation angle on the metal flow field and wall thickness distribution are studied and revealed.

Keywords: Cylinder closure spinning; Tube blank; Finite element simulation; Metal flow; Wall thickness distribution

1 Introduction

Spinning is a special multi-functional processing method, which can achieve stretching, edge turning, binding off and other forming processes [1-2]. As a kind of gas storage container, the gas cylinder has been widely used in industry, mining, military, medicine, diving, automobile and other fields. Stamping is traditionally adopted to form the half of a cylinder, and then the two halves are welded together. However, the dies are needed, and the strength at the weld is low in the traditional process. The gas cylinder produced by spinning can alleviate the defects of joint discontinuity, strength decline, brittle cracking, and greatly improves the air tightness and compressive resistance of the gas cylinder. In addition, in order to ensure the strength and safety of the cylinder, the wall thickness at the neck has thickening requirements, which is difficult to be met by stamping[3].

Many typical cylinder spinning have been carried out by domestic and foreign scholars. In 2007, Xia et al. [4] used the 3D elastic-plastic finite element software MARC to simulate the multi-pass non-axisymmetric tube necking spinning, and studied the stress distribution, thickness reduction, straightness, ellipticity and axial elongation. Liang et al. [5] investigated the forming characteristics of the steel and aluminum alloy cylinder spinning. The wall thickness distribution, stress and spinning force of hot binding off spinning were analyzed by Zhang et al. [6]. Xia Qixiang [7] et al. simulated the single pass necking spinning of the inclined pipes.

Kwiatkowski [8] studied the basic principle of the

neck rotation of the cylinder shape, established a mathematical model to analyze the factors affecting the distribution of the rotation piece wall thickness, and made it clear that the roller path is the main factor affecting the distribution of the wall thickness.

In 2016, Fan Junming and Zhou Qixiong [9] took the gas cylinder as the research object and established the finite element numerical simulation model of the forming process by using the UG drawing software according to the forming characteristics of the material PCrNi3MoVA. They also used the plastic forming analysis software DEFORM to conduct numerical simulation analysis of the spinning closing process, so as to study the stress, strain and spinning in the forming process of the gas cylinder. Takahashi [10] carried out research on cylindrical parts die-free neck compression spinning. Zhu Baohang [11] et al. studied the calculation method of the internal reinforcement height of spinning thin-wall cylindrical parts, and deduced the calculation method of the internal reinforcement height by simplifying the shape of the groove on the core mold and following the principle of constant plastic volume.

Finite element modeling is an effective method to study some key problems in the development of spinning technology, such as strain field and stress field[12-13]. A core idea of this study is to use ABAQUS software to establish the finite element model of the cylinder closing spinning process, and to simulate it numerically. In order to reveal the wall thickness distribution and metal flow of cylinder closure spinning, the finite element model is established, and the simulation results are analyzed.

2 Finite element numerical simulation of the spinning process

2.1 Establishment of the finite element model

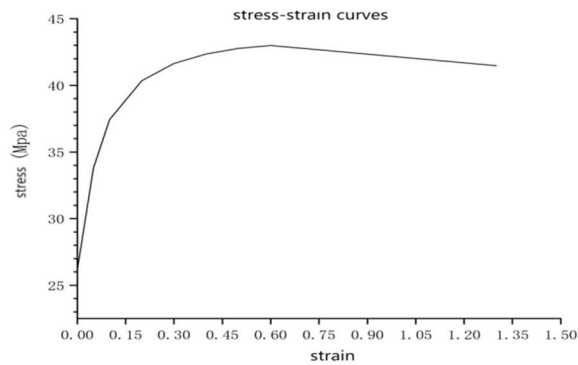


Fig. 1 Stress - strain curve of 6061 aluminum alloy at 200°C

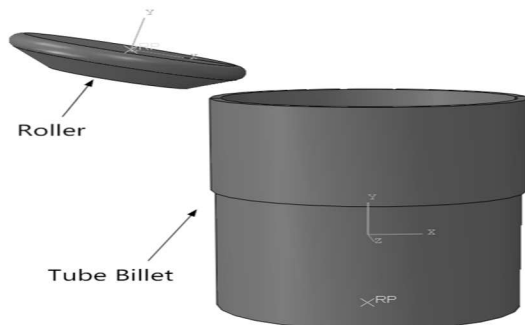


Fig. 2 Assembly effect drawing of 3D model of cylinder closure spinning

The finite element model of the multi-pass cylinder close spinning is established based on the actual productive process. The geometric models of roller and cylinder blank are first established. The inner and outer diameter of the cylinder are 371mm and 398mm respectively, and the length is 195mm. The radius of the roller tip is 15mm, the wheel radius is 150mm, and the thickness is 60mm. The blank material is Al6061

aluminum alloy, and the roller is defined as a rigid body. The density of 6061 aluminum alloy is 2.7g/cm³, the elastic modulus is 67000 MPa, the Poisson ratio is 0.33, and the stress - strain curve at 200°C is shown in Fig.1. The grid of C3D8R cells with eight-node hexahedral cell type is used to mesh the cylinder blank.

The assembly of 3D model of cylinder closure spinning is shown in Fig. 2. According to the actual production experience, the friction coefficient between the blank and the roller is set to 0.2.

2.2 Movement relationship

The movement relationship of the cylinder blank and the roller is controlled through the boundary condition. The cylinder blank is set to rotate at a constant speed of 25r/min. The roller can rotate around its symmetry axis. The passes of the cylinder closure spinning process are conducted for 13, and the roller path diagram is shown in Fig. 3. The path curve of each pass is first discretized into the coordinate point, and then the workpiece coordinate system is transformed into the coordinate under the roller coordinate system with the inclined installation angle. The coordinate value of the wheel path is given to the reference point of the roller, and its movement is controlled according to the path trajectory through the boundary condition. And the displacement of the first pass in the X and Y direction is shown in Tab. 1.

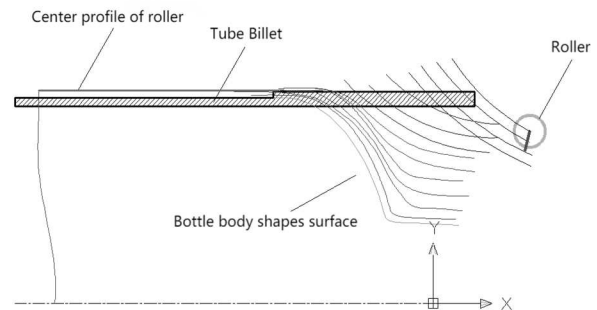


Fig. 3 Track path of multiple cylinder closure

Tab. 1 Displacement amplitude of the roller

Time/s	Amplitude in the X direction / mm	Amplitude in the Y direction / mm
0	0	0
28.226	11.634	-45.582
29.452	11.549	-47.624
30.663	10.775	-49.487
85.726	-42.794	-124.001
89.945	-43.575	-125.877
88.168	-43.609	-127.915
89.396	-43.405	-129.952

3 Simulation results and analysis

3.1 Overview

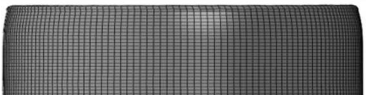
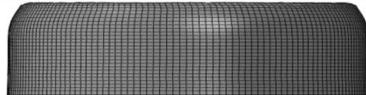
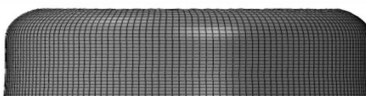
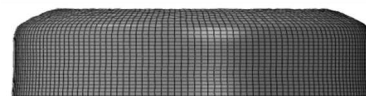
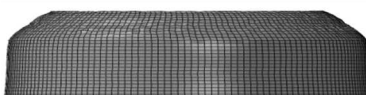
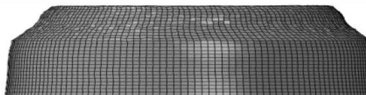
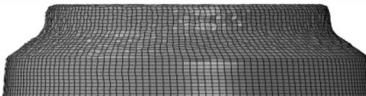
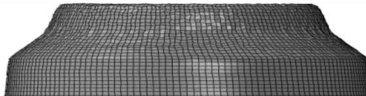
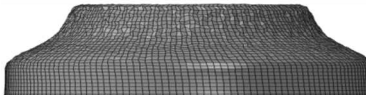
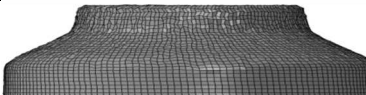
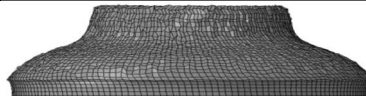
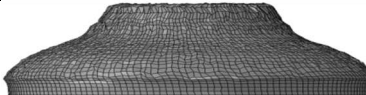
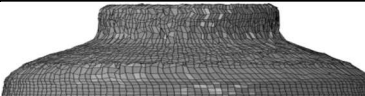
The finite element numerical simulation of the cylinder closure spinning is carried out under the

working conditions in Tab. 2, and the overall situation was analyzed by taking working condition II as an example. A total of 13 passes were simulated for every working condition, and the spinning simulation results after each pass are shown in Fig. 4.

Tab. 2 Simulation working conditions of cylinder closure spinning

Working condition	Roller corner radius / mm	Roller installation angle / °	Roller feed ratios / $\text{mm} \cdot \text{r}^{-1}$	Forward and reverse roller path
I	7.5	15	3.49	Forward
II	15	15	3.49	Forward
III	30	15	3.49	Forward
IV	15	0	3.49	Forward
V	15	25	3.49	Forward
VI	15	15	1.745	Forward
VII	15	15	6.98	Forward
VIII	15	15	3.49	Reverse

Tab. 3 Simulation results after each pass of the multi-roller path under Working II

The number of the multi-roller path	Simulation results
After 1 pass	
After 2 pass	
After 3 pass	
After 4 pass	
After 5 pass	
After 6 pass	
After 7 pass	
After 8 pass	
After 9 pass	
After 10 pass	
After 11 pass	
After 12 pass	
After 13 pass	

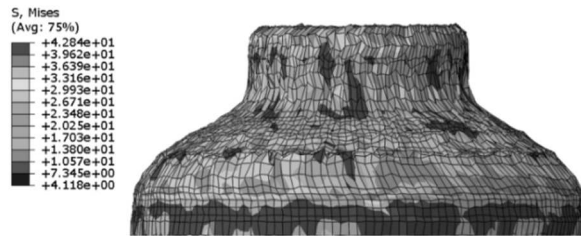


Fig. 4 Stress distribution after 13 passes spinning

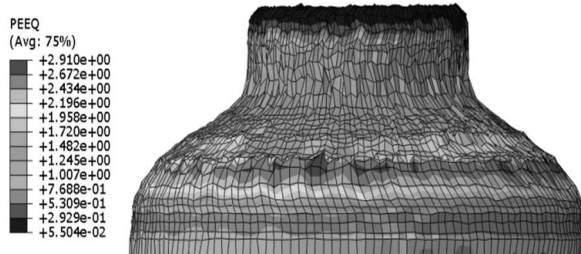


Fig. 5 Strain distribution after 13 passes spinning

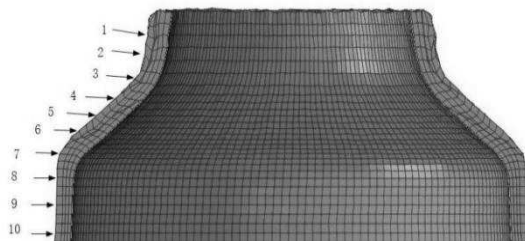


Fig. 6 Location of wall thickness measuring points

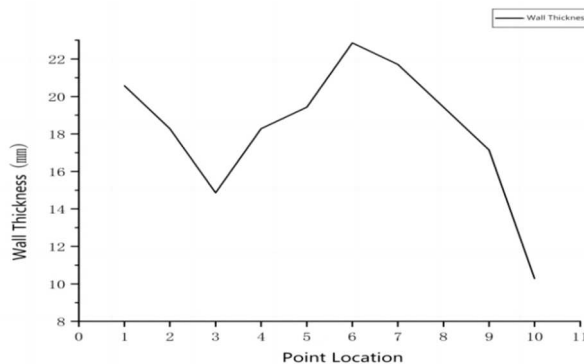


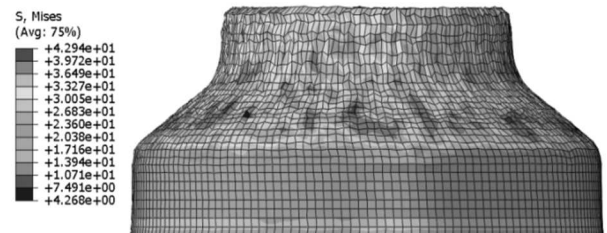
Fig. 7 Wall thickness distribution after 13 passes spinning

It can be found that the end of the spun part presents the shape of the cylinder port with the straight section connected to the hyperbolic bus profile after 13 passes of close spinning. Fig.5 and Fig.6 are the equivalent stress and strain distribution after the final pass. It can be seen that stress concentration is produced in the straight section of the bottle mouth, and the strain increases at the transition from the cone section of the bottle mouth to the straight section of the bottle body. Fig.7 shows the location of the wall thickness measuring points, and the wall thickness distribution of the cylinder section after the final pass is expressed in Fig.8. It can be seen from Fig.8 that the wall thickness reaches the minimum value at point 3, where is the transition from

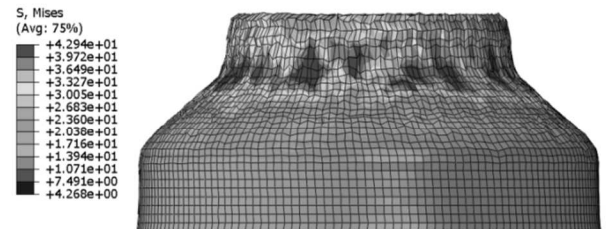
the straight section of the cylinder mouth to the cone section. The maximum stress presents at point 6, where is the transition area from the cone section to the straight section. The wall thickness distribution trend from simulation is consistent with the one from industrial production.

3.2 Effect of the corner radius of the roller

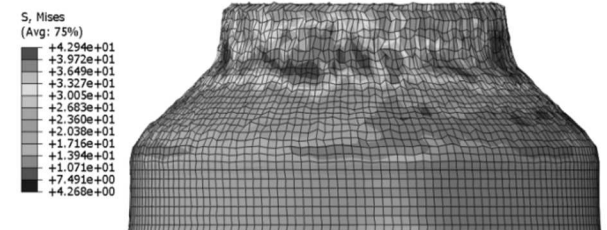
The equivalent stress and strain field of the spun parts with different roller corner radius angles (Working condition I, II, III) after the 10th spinning pass are shown in Fig.9 and Fig.10.



(a) Roller corner radius is 30mm



(b) Roller corner radius is 15mm



(c) Roller corner radius is 7.5mm

Fig. 8 Stress distribution of the spun part using different roller corner radius

As can be seen from Fig. 10, the stress in the straight section of the bottle mouth gradually increases with the decrease of the roller corner radius, but the stress in the cone section of the bottle mouth decreases to a certain extent. The reason is that the larger the roller corner radius has larger deformation contact area in the advance direction, and leads to the greater force exerted on the spinning part. When the conical section is formed, the forward direction of the roller is the opposite direction of the resistance formed in the deformation contact area, so the above theory—the larger the radius of the roller, the larger the stress is fully reflected. However, for the deformation contact area of the straight section is approximately tangent to the direction of the roller, the smaller contact area is easy to cause larger stress.

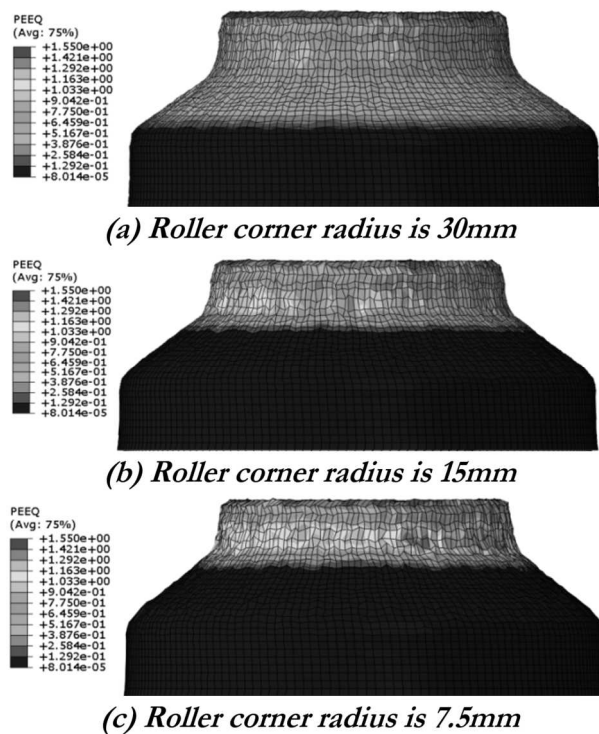


Fig. 9 Strain distribution of the spun part using different roller corner radius

It can be seen from Fig.10 that, the strain of the flat section of the bottle mouth gradually increases with the decrease of the roller corner radius, but the strain of the cone section of the bottle mouth decreases to a certain extent. The reason for this phenomenon is consistent with the stress field distribution: the large deformation stress causes the large deformation in the cone surface section and the straight section respectively.

The wall thickness distribution of the spun parts with different roller corner radius angles (Working condition I, II, III) after the 10th spinning pass are shown in is shown in Fig. 11.

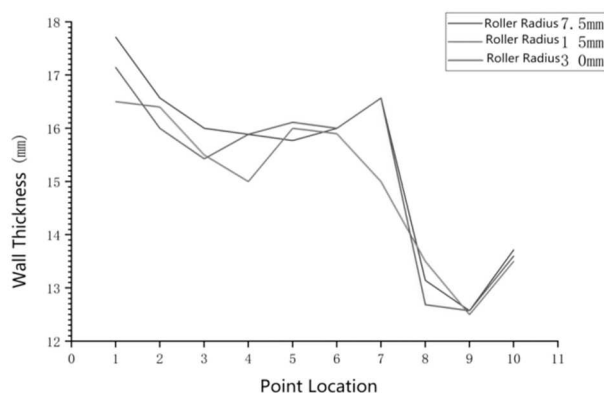


Fig. 10 Spun wall thickness at different roller corner radius

As can be founded from Fig. 11 that, large wall thickness emerges at the straight sections. The wall thickness distribution decreases with transiting to the

cone section, and approaches the original wall thickness of the cylinder blank at 9 and 10 points. It shows that the cylinder closure spinning is a forming process of increasing wall thickness due to the accumulation of metal in the circumference direction. The more metal will be brought out in the moving direction with the greater corner radius, at the same time the circumference metal inflow also gets convenient, so the overall influence of the roller corner radius on the wall thickness distribution is not apparent. The workpiece has the minimum wall thickness at the end of the straight section and the front of the cone section under working condition of 15mm corner radius.

3.3 Effect of roller installation angle

The equivalent stress and strain field of the spun parts with different roller installation angles (Working condition II, IV, V) after the 10th spinning pass are shown in Fig.12 and Fig.13.

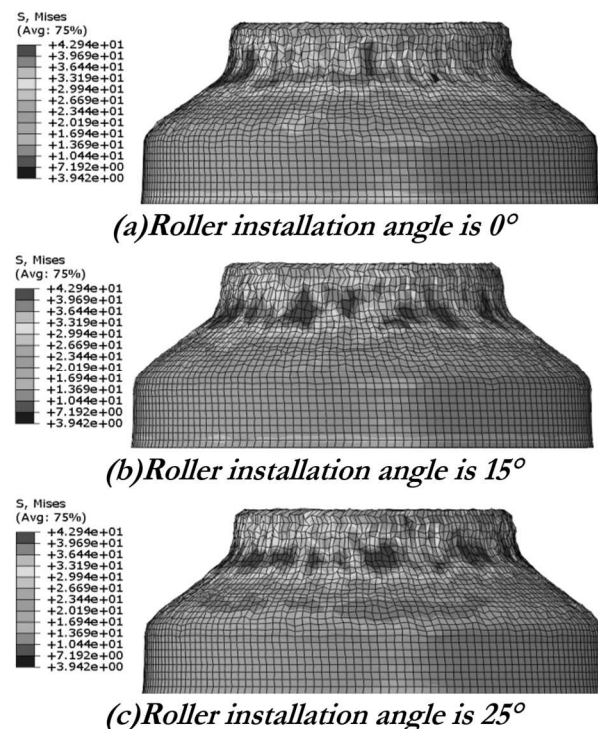


Fig.11 Stress distribution of the spun part using different roller installation angle

As can be seen from Fig.12, the stress distribution is similar under the three working conditions before the roller traveling the conical path. When the conical section is formed, the smaller stress is produced by the working condition of larger installation angle. The strain of the cone section of the bottle mouth gradually increases with the increase of the roller installation angle, and the maximum stain distribution occurs in the working condition with the biggest roller installation angle (see Fig. 13).

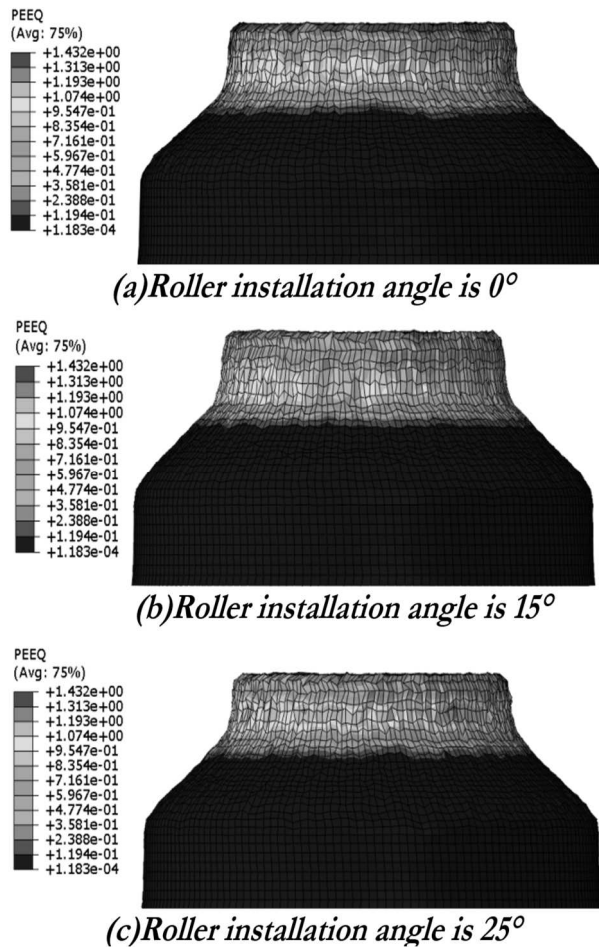


Fig. 12 Strain distribution of the spun part using different roller installation angle

The wall thickness distribution of the spun parts with different roller installation angle (Working condition II, IV, V) after the 10th spinning pass are shown in is shown in Fig. 14.

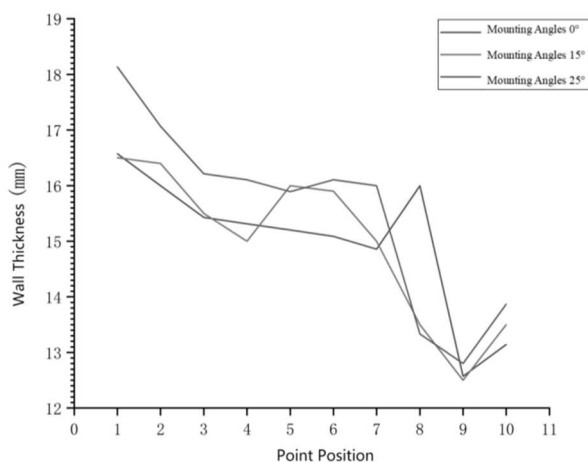


Fig. 13 Spun wall thickness at different roller installation angle

It can be founded from Fig. 14 that, large wall thickness emerges at the straight sections. The wall

thickness decreases with the roller transiting to the cone section, and approaches the original wall thickness of the cylinder blank at 9 and 10 points. The working condition with 25° installation angle has the minimum contact area to form the biggest wall thickness at the section of the straight bottle mouth and cone.

3.4 Effect of roller feed ratios

Under the working condition of 15° roller installation angle and 15mm corner radius, the equivalent stress and strain field of the spun parts with different roller feed ratios (Working condition II, VI, VII) after the 10th spinning pass are shown in Fig. 15 and Fig. 16.

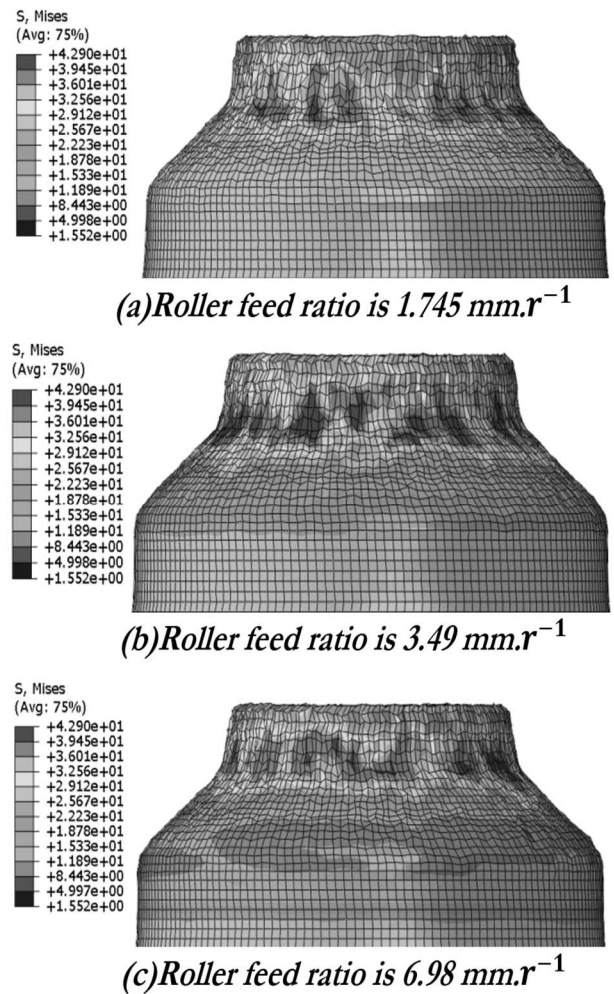


Fig. 14 Stress distribution of the spun part using different roller feed ratios

Fig. 15 shows that, the stress distribution is similar regardless of the roller feed ratio due to the same deformation contact area at the straight section. On the cone section, the larger roller feed ratio will shorten the acting time of the roller on the material with forming the same slope, and smaller stress is retained.

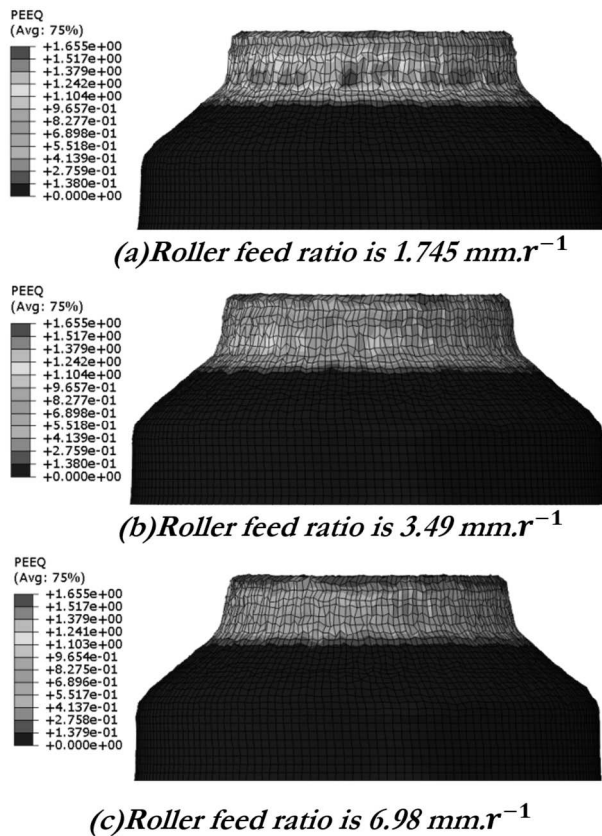


Fig. 15 Strain diagram at different feed ratios

It can be seen from Fig. 16, when the feed ratio increases, there is no obvious change in the strain at the conical section of the bottle mouth, but the strain at the straight section of the bottle mouth gradually decreases, because the metal circumferential extrusion at the straight section is more intense during the dense spinning deformation in unit time.

Under the conditions of 0° , 15° and 25° roller feed ratios, the spun wall thickness distribution after the 10th pass is shown in Fig. 17 which shows that different feed ratios have little influence on the wall thickness formed by cylinder closure spinning.

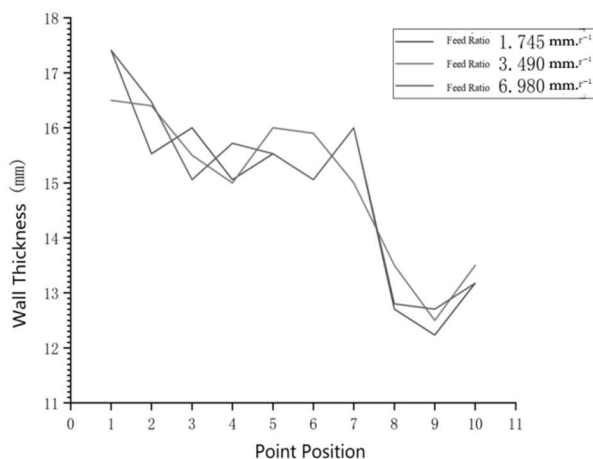


Fig. 16 Spun wall thickness at different roller feed ratios

4 Conclusion

Through the finite element simulation study of the cylinder closure spinning, the influence of different process parameters on the metal flow is obtained as follows:

- The stress and strain in the straight section of the bottle mouth gradually increase with the decrease of the roller corner radius, however, decrease at the cone section. The influence roller corner radius on the wall thickness is not significant.
- The deforming contact area of the straight section of the spun workpiece is similar. In the conical section, the working condition with larger the roller installation angle has smaller stress distribution, and the wall thickness increases with the roller installation angle.
- Stress concentration occurs at the straight section of the bottle mouth, and the stress magnitude is similar with the three feed ratios. The stress in the cone section of the bottle mouth decreases gradually. The strain in the cone section of the bottle mouth changes slightly with the increase of the feed ratio, however, the strain in the straight section of the bottle mouth gradually decreases. The feed ratio in this simulation has little effect on the wall thickness.

References

- [1] LI JING. Analyze the development of rotary-forming technology from the perspective of patent [J]. *China Science and Technology Information*, 2022(23): 19-22. ISSN:1001-8972(in Chinese).
- [2] YANG YU, JIA YANYAN, MAO YAJIE, YANG DONGLIN, ZHENG HONGWEI, ZHANG LEI. Development status and prospect of rotary process [J]. *Light Industry Technology*, 2022,38 (02): 72-74. ISSN : 2095-3518 (in Chinese).
- [3] GIULIANO GILLO, POLINI WILMA. Weight Reduction in an AA2017 Aluminum Alloy Part through the Gas Forming Process of a Blank with a Variable Thickness[J]. *Manufacturing Technology*, 2021,21(2): 192-198. ISSN: 1213-2489.
- [4] XIA Q.X., XIE SH.W., HUO Y.L., RUAN F.. Numerical simulation and experimental

- research on the multi-pass neck-spinning of non-axisymmetric offset tube[J]. *Journal of Materials Processing Tech.*,2007,206(1): 100-121.ISSN: 0577-6686.
- [5] LIANG BAIXIANG, YANG MINGHUI, YANG YIHUI, XIA QIN XIANG. Gas cylinder rotary-forming technology [J]. *Electromechanical Engineering Technology*, 2004 (10): 12-13 + 18-82.:40-44. ISSN : 1009-9492(in Chinese).
- [6] ZHANG TAO, FAN WENXIN, GUO DAIFENG, SHI YONGPENG, LI ZHONG. Study on the mechanical properties of cylinder member rotation [J]. *Thermal workingprocess*, 2017, 46(13): 157-159.ISSN : 1001-3814 (in Chinese).
- [7] XIA QINQIN XIANG, SHANG YUE, ZHANG SHUAIBIN, RUAN FENG. Numerical simulation and test of multi-channel reduced diameter rotation forming of inclined pipe fitting [J]. *Journal of Mechanical Engineering*, 2008 (08): 78-84.ISSN : 0577-6686 (in Chinese).
- [8] L. KWIATKOWSKI, A.E. TEKKAYA, M. KLEINER. Fundamentals for controlling thickness and surface quality during dieless necking-in of tubes by spinning[J]. *CIRP Annals-Manufacturing Technology*, 2013,62(1): 299-302.ISSN: 1726-0604.
- [9] FAN JUNMING, ZHOU QIXIONG. Numerical Simulation on the Hot Spinning Process for Gas Cylinder, *Pressure Vessel Technology*, 2016, 33(5): 39-45.ISSN : 1001-4837 (in Chinese).
- [10] YOICHI TAKAHASHI, SHIGEFUMI KIHARA, TAKUO NAGAMACHI, KOZI HIGAKI. Effects of neck length on occurrence of cracking in tube spinning[J]. *Procedia Manufacturing*, 2018,15.: 1200-1206. ISSN: 2351-9789.
- [11] ZHU BAOXING, ZHAO YIXI, YU ZHONGQI. Calculation method of thin-wall cylinder shape flow rotating inner bar height [J]. *Journal of Plastic Engineering*, 2020,27 (02): 68-78. ISSN: 1001-3539(in Chinese).
- [12] KOREČEK DAVID, SOLFRONK PAVEL, SOBOTKA JIŘÍ. Analysis of the Dual-phase Steel DP500 Stress-strain Characteristics During the Plane Shear Test[J]. *Manufacturing Technology*, 2022,22(1): 34-38.ISSN: 1213-2489.
- [13] KOREČEK DAVID, SOLFRONK PAVEL, SOBOTKA JIŘÍ. Research of Mechanical Properties of the Aluminium Alloy Amag 6000 under the Plane Stress State Conditions[J]. *Manufacturing Technology*, 2022,22(6): 709-712.ISSN: 1213-2489.